

# Geochemistry of Surficial Uranium Deposits from Central Jordan

Hani N. Khoury\*

Department of Geology, Faculty of Science, The University of Jordan, Amman, Jordan

## Abstract

Inhomogeneous unusual surface uranium mineralization hosted by chalk marl/travertine and calcrete/top soil covers large areas in central Jordan. Quarries and trenches with bituminous marl, varicolored marble, travertine and caliche were sampled to understand the geochemistry of the uranium deposits. The samples were characterized mineralogically and chemically using XRD, XRF, SEM, EDX techniques. Relatively high uranium concentrations were found in the calcrete samples where it reaches up to 419 ppm. The secondary uranium mineralization is restricted to the permeable fractured and porous zones. The combustion of the bituminous marl led to the formation of the varicoloured marble in central Jordan. This was followed by the action of circulating highly alkaline water that accelerated the leaching of the redox sensitive trace elements as U and V. Such an alkaline oxidizing environment (pH~12.7) is currently active in Maqarin area, north Jordan. The paleo-circulating water in the combusted rocks of central Jordan oxidized the dissolved  $V^{4+}$  to  $V^{5+}$  and fixed the uranyl-ion as uranyl vanadate. Strelkinite and/or tyuyamunite precipitation and the solid solution, between the two end members, were dependent on the Ca/Na ratio in solution. Carnotite is restricted to the veins associated with the varicoloured marble. The uranyl-vanadate minerals were precipitated from highly alkaline solutions during the dry periods after the precipitation of the thick travertine deposits.

© 2014 Jordan Journal of Earth and Environmental Sciences. All rights reserved

**Keywords:** Surficial uranium minerals, central Jordan, U-V minerals, travertine, calcrete.

## 1. Introduction

Uranium deposits are found in all types of rocks as a result of magmatic, metamorphic and sedimentary processes (Dahlkamp, 1993). Genetic classification of uranium deposits has indicated the exceptional diversity of processes involved in their formation (Cuney, 2009).

Surficial uranium deposits are defined by the International Atomic Energy Agency as young (Tertiary to Recent) near-surface uranium concentrations in sediments or soils (IAEA, 2009). The largest surficial deposits are the calcrete soils and usually cemented by calcium and magnesium carbonates. Such soils form uranium-rich sediments by evapotranspiration process in fluvial to playa systems in a semi-arid to arid climate (Mckay and Mieztis, 2001). Calcrete related uranium deposits occur in valley-fill and in Playa Lake sediments in Western Australia, and at the top of the alluvial sediments in central Namib Desert of Namibia. Uranium is entirely deposited as  $UO_2$  minerals carnotite  $K_2(UO_2)_2(VO_4)_2 \cdot 3H_2O$  and tyuyamunite  $Ca(UO_2)_2(VO_4)_2 \cdot 5-8H_2O$  (Cuney, 2009). Tyuyamunite is closely related to carnotite as indicated by the chemical formula, which is the same except that calcium substitutes for the potassium of carnotite. Strelkinite  $Na_2(UO_2)_2(V_2O_8) \cdot 6H_2O$  is the sodium analogue of carnotite and tyuyamunite.

In central Jordan, unusual surface uranium deposits cover large areas and are mainly associated with the varicolored marble, Pleistocene-Recent travertine and calcrete. Yellow uranium encrustations are also associated with the varicolored marble (pyrometamorphic rocks) and the underlying

bituminous marl (oil shale) and phosphorites (Khoury et al., 2014). The uranium bearing rocks are widely distributed in two areas: Daba (Khan Az-Zabib) and Siwaqa (Fig. 1). The northern boundaries of the first and second areas are located 25 km and 60 km south of Amman with the first area situated between  $E36^{\circ} 00'$  to  $36^{\circ} 15'$  and  $N31^{\circ} 15'$  to  $31^{\circ} 30'$  and the second area between  $E35^{\circ} 00'$  to  $36^{\circ} 15'$  and  $N31^{\circ} 15'$  to  $31^{\circ} 30'$ .

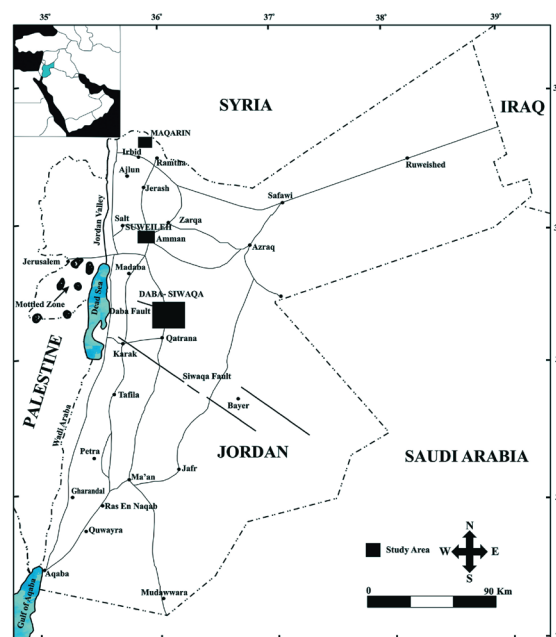
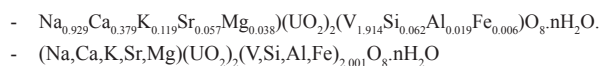


Figure 1: Location map of Daba-Siwaqa area, central Jordan.

\* Corresponding author. e-mail: khouryh@ju.edu.jo

Daba covers 662 sq. km and Siwaqa covers about 660 sq. km. Many tracks leading from the Desert are easily reached from the Amman-Aqaba desert highway, making all parts of the two areas accessible by four wheel-drive vehicles in normal weather. The mean annual precipitation in winter is 110 mm. The mean summer temperature is 23°C with a maximum temperature 44°C and high evaporation rate.

Yellow uranium crystals from the calcrete of central Jordan were analyzed by Healy and Young, (1998) and they found that U-minerals are inhomogeneous and the U and V content ranges are 37- 41%, and 7 – 11% respectively. They concluded a mixed mineralogy of 50% tyuyamunite, 40% tyuyamunite, 5% carnotite with the following mineral solid solution series:



The mineralogy of surficial uranium deposits in central Jordan and uranium source rocks, transport conditions, and deposition processes were explained in detail by Khoury et al., 2014. The geochemistry of uranium and vanadium of the mineral phases was not investigated in detail. The following work aims at understanding the geochemistry of the surficial uranium minerals of central Jordan.

## 2. Geology

### 2.1. Previous Work

Previous work on the varicolored marble from central Jordan has indicated that a multiple phase metamorphism has occurred as a result of spontaneous combustion of the bituminous rocks. The bituminous marl (the non-metamorphic protoliths) varies in composition from argillaceous to siliceous marl. The event is related to the epirogenic movements that took place in late Miocene to Pliocene along the Jordan Rift Valley. The Miocene tectonism and/or a meteorite impact were most probably the triggering factor which initiated the metamorphic event in central Jordan. Recently a large meteoritic impact structure has been discovered in Jabal Waqf as Suwwan, some 30 km east of the marble (cement) area (Salameh, et al., 2006, 2008).

The event was not simultaneous and was not one event (Khoury and Nassir, 1982 a, b; Khoury et al., 1984; Khoury, 1989; Khoury et al., 1992). The product minerals reflect the chemical composition of the original bituminous marl. The mineralogy of the marble is comparable to that of cement clinker (high temperature assemblage) and to hydrate cement products (low temperature assemblage). The high temperature mineral assemblage includes among others: diopside, wollastonite, monticellite, gehlenite-akermanite, spurrite, and merwinite, garnet, anorthite, pervoskite, magnesioferrite, fluorapatite and recrystallized calcite. The low temperature assemblage includes among others: calcium silicate hydrates (tobermorite, jennite, afwillite, apophyllite), sulfates (ettringite, hashemite, barite, thaumasite, gypsum), stable and metastable carbonates (calcite, vaterite, aragonite, kutnahorite), oxides and hydroxides (goethite, portlandite, hydrocalumite), and many calcium silicate hydrates (Khoury and Nassir, 1982a, b). The mineralogy of similar areas in Israel was recently reviewed by Gellerhe et al., 2012. They concluded that isochemical reactions took place as

a result of the combustion of the organic matter. They compared between the different metamorphic rocks and their bituminous marl equivalents using the three component system  $\text{Al}_2\text{O}_3\text{-SiO}_2\text{-CaO}$  and isocon plots. The average mass loss of 30% of the protolith volume was the result of oxidation and decarbonation processes. The oxidation of the organic matter during combustion has led to an average mass loss of 30% and some volume loss as a result of dehydration and decarbonation processes. The stable isotopes ( $\delta^{18}\text{O}$  and  $\delta^{13}\text{C}$ ) were depleted from the carbonates (recrystalline calcite, spurrite and larnite). The isotopic depletion in  $\delta^{18}\text{O}$  and  $\delta^{13}\text{C}$  from equilibrium values supports the thermal event (Clark et al., 1993; Khoury, 2012). A similar type of travertine forming from highly alkaline waters has been observed in Oman (Clark et al., 1992; 1993). A mud-volcanic hypothesis was suggested by Sokol et al., (2007; 2008; 2010), Sharygin et al., (2008); Vapnik et al., (2007) for the origin of the marble of the mottled zone. The active metamorphism in Maqarin area, north Jordan however, supports the combustion model (Khoury and Nassir, 1982b).

### 2.2. Geology of the studied area

The studied area was mapped in details by the Natural Resources Authority (NRA) (Barjous, 1986; Jasser, 1986). The geology, stratigraphy and sedimentology of central Jordan were described in details (Powell, 1989, Powell and Moh'd, 2011). The exposed rocks are sedimentary and range in age from Upper Cretaceous (Turonian) to Tertiary (Eocene). Outcrops in central Jordan illustrate the presence of three main rock types: Bituminous marl; varicolored marble (pyrometamorphic rocks); travertine and calcrete. The Bituminous Marl Unit overlies the Phosphorite Unit and underlies the varicolored marble and all are of Maestrichtian – Lower Paleocene age. Recent work of Alqudah et al., 2014 and 2015 has indicated that the bituminous marl of central Jordan contain abundant calcareous nannofossil taxa of Eocene age along with varying abundances of Maestrichtian and Paleocene taxa that suggests major reworking. Travertine and calcrete deposits are of Pleistocene – Recent age. They found up to 60 m thick succession of Early Eocene bituminous marl.

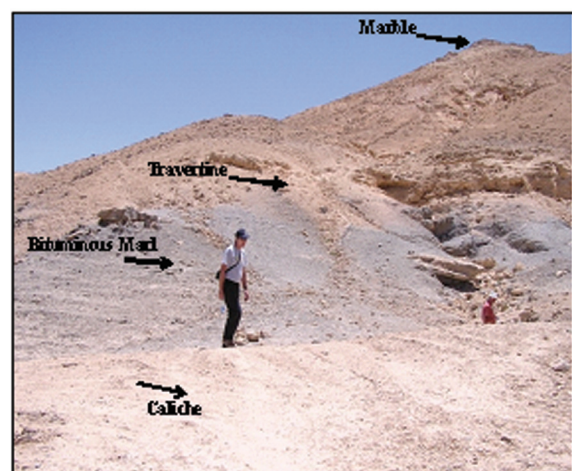
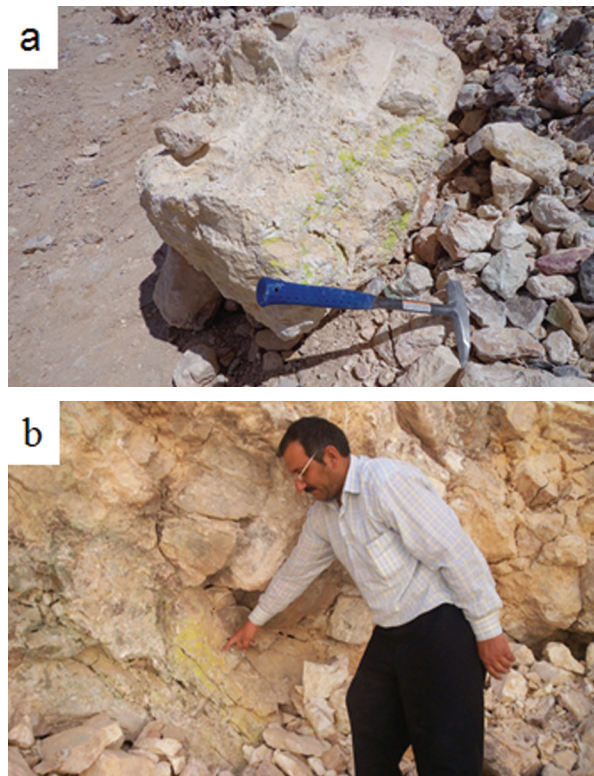


Figure 2: An outcrop in central Jordan illustrating travertine, caliche, bituminous marl and marble.

Figure 2 illustrates the different lithological units' that crop out in central Jordan. The thickest outcrop (up to 30 m) is found on the downthrown side of Siwaqa fault. Gentle folding and faulting that trend NW-SE and E-W are the main structures. In Jordan, synsedimentary uranium deposits are formed during sedimentation of bituminous marl (oil shale) and phosphorites in shallow continental shelves. Jordan was part of the phosphorite belt along the southern margin of the Tethys Ocean (paleolatitude 8–15° N), (Cuney, 2009; Abed, 2012). Uranium concentration values range between 60-379 ppm (parts per million or g/ton) with an average value of 153 ppm. Certain phosphorite horizons in central and south Jordan have higher U values than the average and reach up to 242 ppm (Abed, 2012). The phosphorites of Jordan are carbonate fluor-apatite (francolite) with a structural formula  $[Ca_{9.86}Mg_{0.005}Na_{0.14}][PO_{4.93}CO_3 1.07 F_{2.06}]$  (Abed and Fakhouri, 1996). Uranium substitutes for Ca in the carbonate fluor-apatite structure and correlates well with Ca in the Jordanian phosphorites (Abed, 2012; Khoury et al., 2014). The travertine and calcrete that host the main uranium deposits overlie the varicolored marble (pyrometamorphic rocks) in all the studied outcrops. Secondary clay smectite fillings (volkonskoite) are mainly responsible for the green color of the travertine and calcrete (Khoury, et al., 2014; Khoury and Zoubi, 2014). Apatite, barite, hashemite, ettringite, tobermorite and opaline phases are also present as secondary minor phases (Khoury, 2012).

### 2.3. Field and laboratory work

Most of the field work was done during summer of 2011 and 2012. Sampling has concentrated on outcrops from the quarries and trenches excavated by the private sectors and/or the Natural Resources Authority. Samples were collected from the bituminous marl, varicolored marble, intermixed chalk marl/travertine and calcrete/top soil outcrops.



**Figure 3:** a-f. Secondary yellow uranium encrustation in (a) black marble (b) highly altered marble (c) travertine (d) calcrete (e) Cr - rich plant molds in travertine (f) varicolored marble breccia embedded in travertine.

The bituminous marl is highly fractured and is affected by the alkaline circulating water as indicated by the secondary minerals (mainly secondary carbonates and sulfates) filling the cracks and cavities. Few outcrops of the varicolored

marble are not altered (Fig. 3a). The highly altered marbles by the alkaline circulating water are characterized by low temperature minerals filling fractures as hydrous Ca-silicates and Al-silicates (Fig. 3b). The travertine thickness in the studied areas reaches up to 30 meters. The outcrops are white yellow – brown and are characterized by wavy, vesicular, banded structure and are composed of calcite with mineralized plant remains and other secondary minerals. Secondary U- and V-rich phases are present as yellow encrustations and filling voids, cavities and along bedding planes in travertine (Fig. 3c, d). Few intermixed chalk marl/travertine and calcrete/top soil outcrops show the association of uranium encrustations and green Cr-rich smectite. Plant molds and replacement of vegetation by Cr-rich minerals are typical for central Jordan travertine (Fig. 3e). The calcrete is massive hard to nodular and sometimes friable to white, with voids and fractures. It varies in color between pale brown to creamy to white. The earthy calcrete as observed in the trenches forms a fairly continuous layer that grades upwards into the overlying regolith. The hard porous calcrete is intermixed with gypsum in many trenches. Secondary green Cr-rich smectite and yellow uranium

encrustations are common (Fig. 3e). Brecciated varicolored marbles are noticed associated and embedded in travertine cement (Fig. 3f). The chalk marl/calcrete and/or travertine/top soil are underlain by baked bituminous limestone and or varicolored marble.

Thirty five bituminous samples of the varicolored marble, travertine and calcrete were collected and are described in Table 1. Fifteen samples were collected from quarries and trenches of Siwaqa area (Q and T samples) and twenty from Daba quarries (KH samples). Another ten selective samples of yellow encrustations were also collected from two trenches excavated by Areva Co. (N 31° 23' 361", E 36° 11' 361") and Natural Resources Authority (NRA) (N 31° 31' 643", E 36° 12' 301"). Figure 3(a-f) illustrates some of the uranium rich outcrops.

All samples were subjected for mineralogical and chemical characterization. Polished thin sections were prepared for all the samples at the Department of Earth Sciences, University of Ottawa, Canada. Part of the analytical work was carried out using X-Ray fluorescence spectrometer (XRF), scanning electron microscope (SEM) and X-Ray diffractometer (XRD)

**Table 1:** Description of the samples from central Jordan and the XRD results (Khoury, 2012).

Sample No.	Description	XRD Results
KH01	Baked bituminous marl	Calcite*, gypsum, illite/smectite, francolite
T2-1	Bituminous limestone	Calcite*, gypsum, illite/smectite
KH02	Black marble	Calcite*
KH03	Pale green marble (altered)	Calcite*, smectite, francolite
KH04	Gray marble	Calcite*, apatite, smectite
KH05	Yellow marble	Calcite, wollastonite, aragonite
Q-1	Porous travertine with green clay	Calcite*, Cr-smectite
Q-2	Porous travertine with green clay	Calcite*, Cr-smectite
Q-3	Porous travertine with green clay	Calcite*, Cr-smectite
Q-4	Porous travertine with green clay	Calcite*, Cr-smectite
Q-5	Porous travertine with green clay	Calcite*, Cr-smectite
Q-6	Porous travertine with green clay	Calcite*, Cr-smectite
Q-7 old	Porous travertine with green clay	Calcite*, Cr-smectite
KH06	Travertine with green clay	Calcite*, Cr-smectite, francolite
KH07	Travertine with green clay	Calcite*, Cr-smectite, francolite
KH08	Travertine with green	Calcite*, francolite
KH09	White travertine	Calcite*
KH10	Travertine	Calcite*, Cr-smectite, francolite
KH18	Green soft travertine	Calcite*, quartz, smectite
KH19	Green travertine	Calcite*, quartz, smectite
KH20	Green travertine	Calcite*, quartz, opal-CT
KH21	Green travertine	Calcite*, quartz, opal-CT
KH22	Green travertine	Calcite*, gypsum, opal-CT, Cr-smectite
KH23	Green travertine	Calcite*, opal-CT, Cr-smectite, gypsum
T2-3	Yellowish gypsum rich calcrete with green clay	Calcite, gypsum, Cr-smectite
T3-4	Yellowish gypsum rich calcrete with green clay	Calcite*, gypsum, ettringite, Cr-smectite
T3-5	Yellowish gypsum rich calcrete with green clay	Calcite*, gypsum, Cr-smectite
T2-6	Dolomite rich caliche with green clay	Calcite*, gypsum, Cr-smectite
T4-1	Red calcrete with green clay	Calcite*, Cr-smectite
T5-1	Yellowish calcrete with green clay	Calcite*, gypsum, ettringite, Cr-smectite
T5-2	Green yellow calcrete	Calcite*, gypsum, Cr-smectite

(\*): major component

in the laboratories of the Federal Institute for Geosciences and Natural Resources, Hanover (BGR), the Geology Department, Greifswald University, Germany and Mango Center, University of Jordan. Most of the work (XRD, SEM, EDX, and Microprobe) was accomplished at the Department of Earth Sciences, University of Ottawa. A JEOL 8230 Super Probe for quantitative chemical analyses and images of minerals was used. The electron microprobe is fitted with five WDS spectrometers and a high count-rate silicon drift detector (SDD) EDS spectrometer. A JEOL 6610LV SEM was also used for studying and analyzing the uranium phases. All uranium rich samples were investigated for single crystal EDS analysis where hundreds of spot EDS analyses were accomplished. The XRD is a Philips double goniometer X'Pert system with *CuK $\alpha$*  radiation. The whole rock 'random powder' samples were scanned with a step size of  $0.02^\circ$  2 theta and counting time of 0.5 s per step over a measuring range of  $2$  to  $65^\circ$  2 theta. Powdered samples were chemically analyzed using a PANalytical Axios and a PW2400 spectrometer available in BGR. Samples were prepared by mixing with a flux material and melting into glass beads. The beads were analyzed by wavelength dispersive x-ray fluorescence spectrometry (WD-XRF). The loss on ignition (LOI) was determined by heating 1000 mg of each powdered sample to  $1030^\circ\text{C}$  for 10 min. After mixing the residue with 5.0 g lithium metaborate and 25 mg lithium bromide, it was fused at  $1200^\circ\text{C}$  for 20 min. The calibrations were validated by analysis of Reference Materials. «Monitor» samples and 130 certified reference materials (CRM) are used for the correction procedures.

### 3. Results

Tables 1, 2 and 3 represent the mineralogical and chemical composition of the different rock varieties. Table 1 describes the samples and their mineral content as indicated from the XRD results. The petrographic results indicated that the bituminous marl is biomicrite with 10% average clay content. Clay minerals are mostly highly expansive mixed layer illite/smectite. In addition to micritic calcite, francolite (fluor-carbonate apatite) and dolomite are the essential constituents of the rocks. Framboidal pyrite, other sulfides, rare earth minerals and organic matter are found filling the forams cavities and intermixed with the matrix. The photomicrographs of Fig. 4 describe the laminated biomicritic texture, the bioclasts and the rare earth minerals of the bituminous marl. The EDS results of rare earth minerals vary in their crystal chemistry (Fig. 4d). Some crystals are composed of  $\text{Y}_2\text{O}_3$  (15.2%-24.8%),  $\text{V}_2\text{O}_5$  (18.8%-20.30%) and  $\text{Fe}_2\text{O}_3$  (2.5%-16.20%). Some crystals have additional  $\text{Nd}_2\text{O}_3$  (2.1%-4.6%) and  $\text{CeO}_2$  (7.5%-7.8%). Detrital quartz, K-feldspar and mica are also present. Traces of Zn, Cu, Ni, Fe sulfides and selenides, native selenium, sulphates and selenates, and goethite are also present. In the equivalent bituminous rocks in north Jordan (Maqarin) pyrite, other sulfides and selenides as sphalerite, galena, Ni-Se, Ag-Se, AgCuNiFeZnCd-S-Se, FeCuZnNi-S, ZnCuFeNi-S and ZnFeCuNi-Se were reported (Milodowski et al., 1998).

Table 2 illustrates the chemical composition of the major elements that agrees with the XRD results. The XRD results have indicated that calcite is the major mineral in all rock varieties. Gypsum and mixed layer illite-smectite are present

in the bituminous marl. Wollastonite, calcite, aragonite, and francolite are among the minerals associated with the marble. Gypsum, ettringite, hashemite, opal CT, quartz, francolite, Cr-smectite, fluorite and halite are among the secondary minerals in the travertine and calcrete.

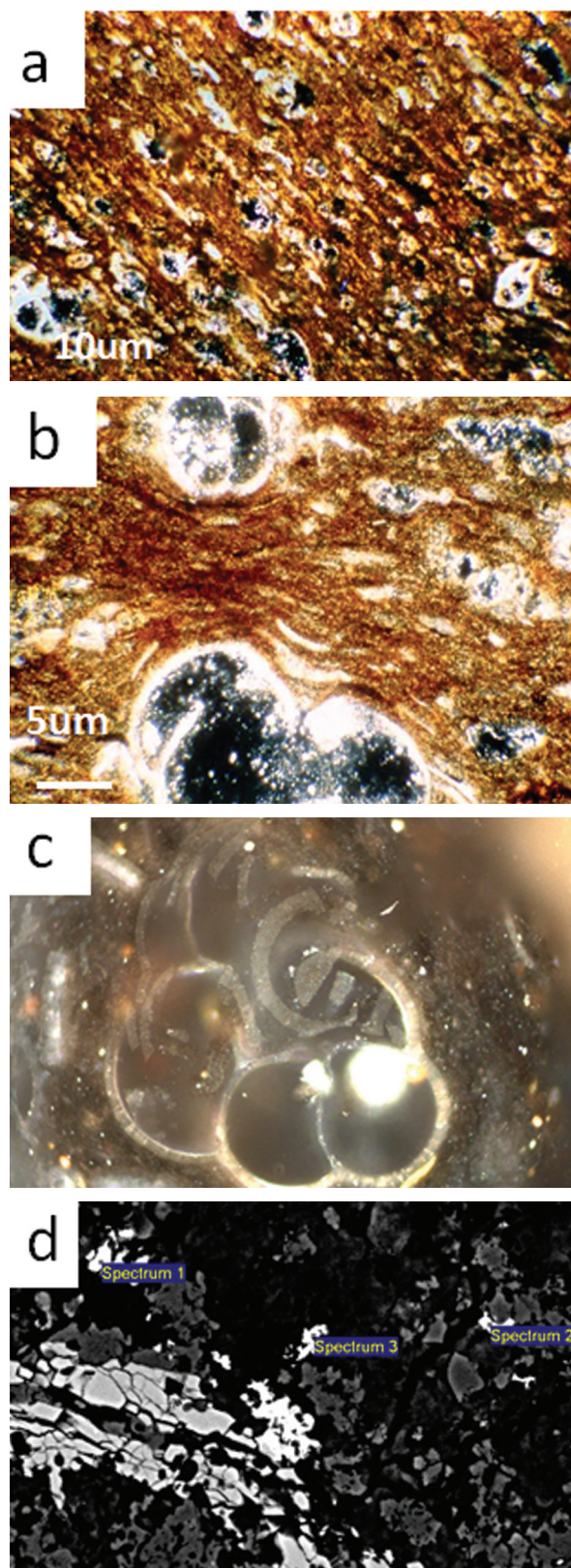


**Figure 4:** Photomicrographs of bituminous marl (a) silt-size bioclasts embedded in a laminated organic-rich matrix (b) fossil shell fragments filled with organic matter (c) bioclasts (forams) in micritic matrix (d) rare earth minerals in micritic matrix (Khoury et al., 2014)

**Table 2:** Chemical composition (%) of bituminous marl, marble, travertine and calcrete (Khoury, 2012).

Sample No	SiO <sub>2</sub>	Al <sub>2</sub> O <sub>3</sub>	Fe <sub>2</sub> O <sub>3</sub>	MgO	CaO	Na <sub>2</sub> O	K <sub>2</sub> O	P <sub>2</sub> O <sub>5</sub>	SO <sub>3</sub>	F	LOI	Total
<b>Bituminous marl</b>												
KH01	18.89	2.45	1.0	0.65	39.35	0.16	0.105	4.731	0.3	0.66	30.15	98.57
T2-1	36.04	7.58	2.67	2.13	19.56	0.943	0.471	1.793	nd	0.29	16.13	87.6
<b>Varicolored marble</b>												
KH02	1.24	0.18	0.15	1.02	53.06	<0.01	<0.005	0.538	0.13	0.17	42.6	99.14
KH03	5.88	1.96	0.58	1.38	48.08	0.05	0.006	0.893	0.73	0.22	39.01	98.89
KH04	2.64	0.66	0.44	0.69	51.52	0.05	0.008	1.624	0.43	0.28	40.47	98.89
KH05	25.45	7.27	2.35	1.75	35.48	0.21	0.068	1.622	0.4	0.14	24.02	99.11
<b>Travertine</b>												
Q1	10.17	2.8	1.02	0.81	42.72	0.282	0.042	0.731	nd	nd	34.33	92.9
Q2	15.37	4.19	1.39	1.378	35.89	0.513	0.103	1.192	nd	0.24	29.71	90.0
Q3	11.71	3.33	0.98	1.093	41.51	0.429	0.044	0.986	nd	0.14	33.29	93.5
Q4	16.58	4.38	1.12	1.55	36.18	0.242	0.035	0.875	nd	0.01	30.01	91.0
Q5	17.63	3.22	0.61	2.603	36.46	0.195	0.03	8.063	nd	1.16	22.60	92.6
Q6	11.78	2.69	0.60	1.895	42.82	0.156	0.034	8.63	nd	1.08	25.83	95.5
Q7	27.39	4.03	0.59	2.232	21.02	1.028	0.23	1.231	nd	0.1	19.66	77.5
KH06	12.08	2.07	0.35	1.19	41.01	0.29	0.061	2.946	0.44	0.4	34.61	95.75
KH07	17.0	2.94	0.4	1.45	34.10	0.57	0.08	2.987	0.47	0.4	32.7	93.53
KH08	2.30	0.56	0.39	0.23	52.55	0.07	<0.005	4.645	0.66	0.57	37.46	99.51
KH09	11.88	0.08	0.07	1	47.27	<0.01	<0.005	0.166	0.26	0.12	38.34	99.18
KH10	4.09	1.26	0.49	0.73	50.21	0.06	<0.005	3.33	0.47	0.42	38.18	99.34
KH18	41.26	0.3	0.06	0.68	29.81	0.07	0.009	0.147	0.16	0.18	25.93	98.62
KH19	43.56	0.1	0.01	0.8	28.72	0.06	0.006	0.024	0.16	0.13	24.92	98.49
KH20	41.99	0.11	<0.01	0.54	29.59	0.07	0.034	0.024	0.22	0.08	26.2	98.89
KH21	35.25	0.13	<0.01	0.41	33.67	0.07	0.02	0.256	0.1	0.11	28.99	99.01
KH22	47.14	0.08	0.01	0.57	26.04	0.13	0.006	0.075	0.96	0.1	23.68	98.82
KH23	36.85	0.54	0.17	0.4	31.17	0.03	0.017	0.472	0.94	0.17	28.15	98.93
<b>Calcrete</b>												
T-4	4.99	0.83	0.26	0.458	50.49	0.042	0.004	0.914	nd	0.31	39.49	97.8
T2-2	2.69	0.92	0.298	6.276	44.79	0.033	0.008	0.207	nd	nd	42.34	97.6
T5-2	4.95	1.5	0.542	0.668	31.97	0.207	0.044	0.771	13.44	0.22	9.36	63.7
T2-3	11.36	1.7	0.368	2.161	28.3	0.402	0.073	1.093	2.6	nd	12.44	60.6
T3-4	5.13	1.56	0.305	0.637	31.88	0.368	0.035	1.106	20.52	0.19	12.08	73.8
T3-5	19.93	3.3	0.893	3.882	27.56	0.665	0.155	4.84	6.02	0.55	15.13	82.9
T5-1	20.03	6.09	1.381	5.761	24.98	1.087	0.088	4.196	1.24	0.81	18.74	84.4
T2-6	18.11	2.06	0.278	2.924	26.34	0.588	0.085	0.488	4.15	nd	21.91	76.9

The chemical composition of the studied samples illustrate that CaO is the main oxide (highest value = 51.5%) and is mainly related to the presence of calcite. The highest SiO<sub>2</sub> value (47.14) is related to the opaline phases found in travertine. The highest MgO, Fe<sub>2</sub>O<sub>3</sub> and Al<sub>2</sub>O<sub>3</sub> values (2.1%, 2.6% and 7.6% respectively) are found in the bituminous marl and are related to clay minerals. The highest P<sub>2</sub>O<sub>5</sub> (8.6%) and F (1.1%) are found also in travertine and are related to the presence of francolite and fluorite. The trace elements composition is given in Table 3. The table illustrates that all samples are enriched in redox sensitive trace elements as U, Cr, V, Zn, and Ni. The highest trace elements content is present in the calcrete samples. The wide range of trace elements composition in the whole rock samples indicates a non-homogeneous distribution because the yellow and green mineralization of the secondary minerals is restricted to voids, fractures and bedding planes. The green travertine with Cr-smectite has the highest Cr content that reaches up

to 4.1%. Strontium substitutes for calcium in the carbonates and francolite. Cr, Ni, U, V, Zn and Zr are associated in the different sulphide-selenide mineral phases. The U values in the whole rock samples of the bituminous marl, varicolored marble, travertine and calcrete range between 32-34 ppm, 6-17 ppm, <3-52 ppm and 6-419 ppm respectively. The highest uranium concentration (419 ppm) is found in a surface calcrete sample (T2-6). The V values in the whole rock samples of the bituminous marl, varicolored marble, travertine and calcrete range between 429-558 ppm, 21-196 ppm, 27-1117 and 62-7136 ppm respectively. The highest V concentration (0.74%) is in a surface calcrete sample (T5-1). The high V values are related to its incorporation in phases other than uranium vanadate.

The chemical composition of hundreds of spotted crystals has revealed 10 varieties of uranium phases. The results are summarized in Table 4. The EDS spot analyses of polished thin sections were carried out on crystals associated with

calcrete and aggregates associated with travertine (Fig. 5). Hundreds of spotted selected uranium crystals and aggregates with EDS are illustrated in Fig. 6 (a-j). The results are summarized in Table 4. The table illustrates the variability in the chemistry of the surficial uranium minerals. The U-V minerals are the most common in the Areva and NRA uranium rich trench samples. Fig. 7 illustrates the positive correlation between  $UO_3$  and  $V_2O_5$  that confirm their presence in the same phase. The high  $V_2O_5$  values in some crystals are related to the dominance of  $V_2O_5$  in the structure. The low correlation coefficient between U and V in the whole rock samples (Fig. 8) is related to the presence of V in the structure of other minerals in the travertine and calcrete. The XRD results have indicated that metatuyuyamunite  $Ca(UO_2)_2V^{5+}2O_8 \cdot 3(H_2O)$  and strelkinite  $Na_2(UO_2)_2V_2O_8 \cdot 6(H_2O)$  are the main uranium vanadate minerals. All possible solid solution between the two end members is also present (Fig. 9). The XRD

results have also indicated the occurrence of a vanadium free carbonate phase urancalcarite  $Ca(UO_2)_3(CO_3)(OH)_6 \cdot 3H_2O$ . Table 4 indicates also the presence of other minerals as carnotite  $K_2(UO_2)_2V_2O_8 \cdot 3(H_2O)$  and other unidentified varieties (carbonates -silicates) that need further studies. Carnotite is found as a minor constituent associated with the marble and depends on the availability of K as indicated by the presence of secondary K-apophyllite (Fig. 10). Carnotite is found in brown marble as yellow - green encrustations restricted to the secondary veinlets. Table 4 illustrates also the presence of other phases with: U and V - possibly ferganite  $U_3(VO_4)_2 \cdot 6H_2O$ ? ; U and V and low Ca silicate; U and V with high Ca silicate; U, V, and Na carbonate; U and V, Na silicate-carbonate; only U and Ca possibly vorlanite  $(CaU^{6+})O_4$ . All varieties are associated with altered marble, travertine and calcrete with the exception of the last variety with no vanadium that is restricted to unaltered marble.

**Table 3:** Trace elements composition (ppm) of bituminous marl, marble, travertine and calcrete.

Sample No	Cr	Ni	Sr	U	V	Zn	Zr
<b>Bituminous marl</b>							
KH01	3552	361	1043	32	558	1860	33
T2-1	594	93	575	34	429	347	118
<b>Range</b>	<b>594-3552</b>	<b>93-361</b>	<b>575-1043</b>	<b>32-34</b>	<b>429-558</b>	<b>347-1860</b>	<b>33-118</b>
<b>Varicolored marble</b>							
KH02	174	24	656	7	21	124	10
KH03	2612	92	748	6	135	374	17
KH04	621	245	742	17	46	877	10
KH05	583	198	2177	17	196	135	53
<b>Range</b>	<b>174-2612</b>	<b>24-245</b>	<b>656-2177</b>	<b>6-17</b>	<b>21-196</b>	<b>124-877</b>	<b>10-53</b>
<b>Travertine</b>							
Q-1	17636	124	440	9	124	538	37
Q-2	23888	317	419	13	165	688	51
Q-3	15797	212	484	10	136	483	47
Q-4	15937	242	819	9	142	246	79
Q-5	24641	278	601	38	193	418	66
Q-6	12660	162	734	37	125	453	80
Q-7	74621	190	601	33	1117	265	75
KH06	26379	105	619	34	473	253	38
KH07	41156	163	666	31	657	634	40
KH08	272	31	266	25	27	264	22
KH09	49	3	147	16	46	993	9
KH10	70	145	483	17	68	778	32
KH18	5450	34	129	52	96	718	9
KH19	6317	36	97	48	84	600	<3
KH20	4022	13	105	21	51	259	6
KH21	2469	13	130	19	39	218	7
KH22	5035	24	101	16	63	337	5
KH23	3284	92	119	42	59	448	10
<b>Range</b>	<b>49-74621</b>	<b>3-317</b>	<b>97-819</b>	<b>9-52</b>	<b>27-1117</b>	<b>218-993</b>	<b>&lt;3-80</b>
<b>Calcrete</b>							
T-4	531	44	406	6	62	400	28
T5-2	4723	205	381	86	2024	223	47
T2-3	26060	152	466	41	5236	3761	46
T3-4	26600	94	748	77	7444	287	46
T3-5	28914	301	597	41	4218	1229	80
T5-1	19967	1095	1095	33	9520	1604	114
T2-6	63171	107	727	419	7137	208	44
T2-1	594	93	575	34	429	347	118
<b>Range</b>	<b>531-6317</b>	<b>44-1095</b>	<b>381-1095</b>	<b>6-419</b>	<b>62-7137</b>	<b>208-3761</b>	<b>28-118</b>

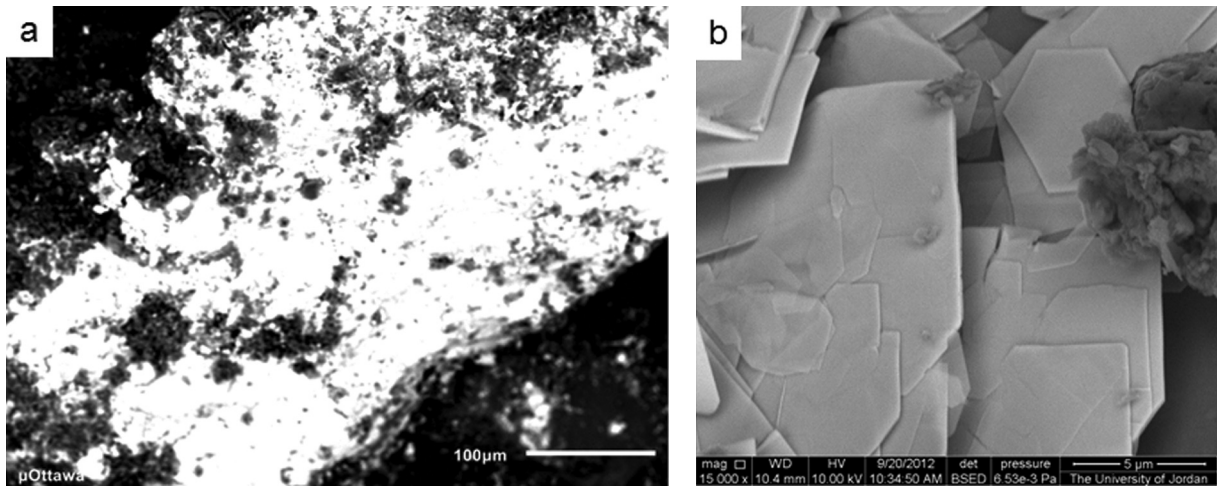


**Figure 5:** Yellow uranium (metatyuyamunite-strelkinite (a) aggregates associated with travertine (b) orthorhombic crystals associated with calcrete.

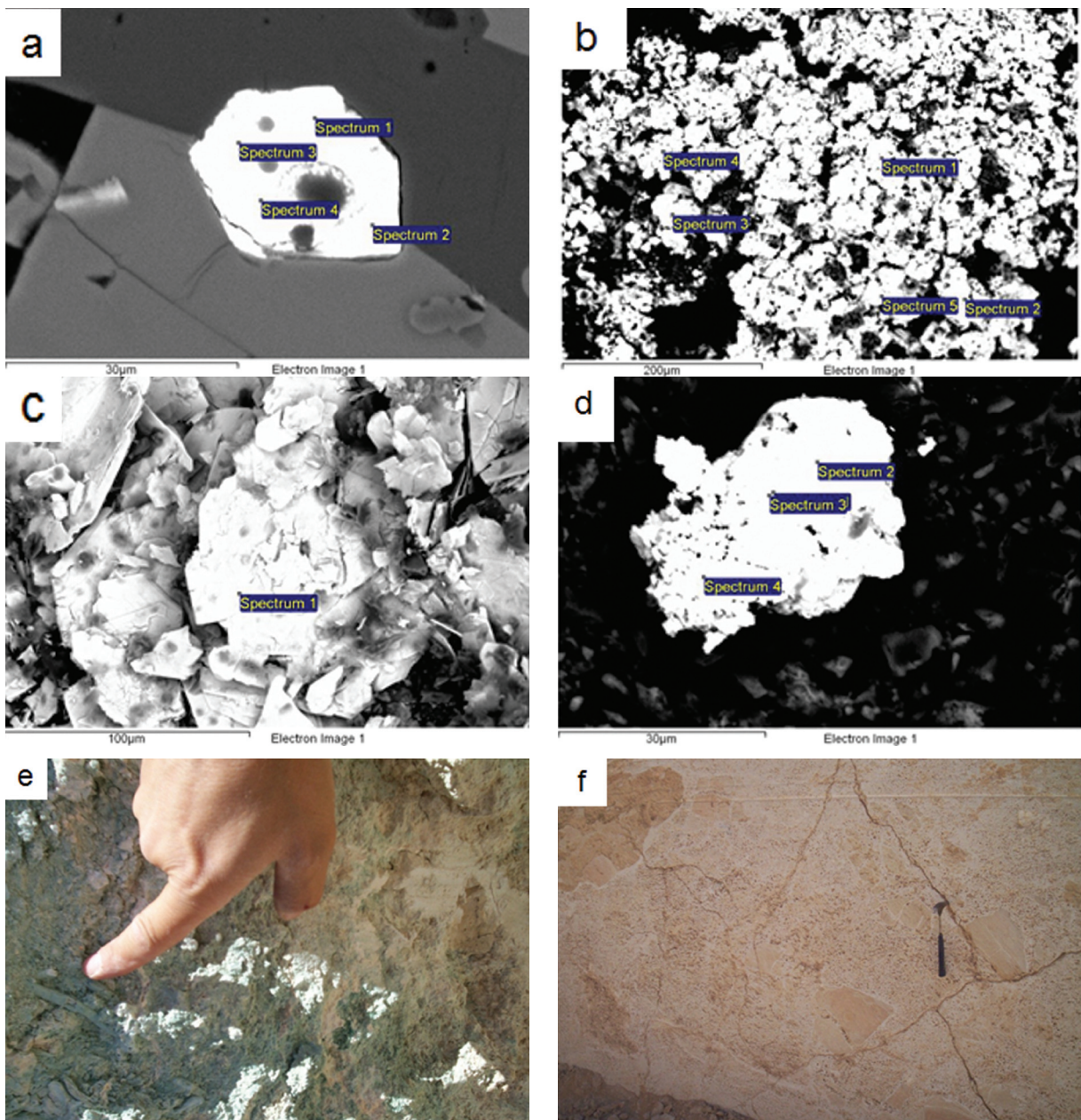


**Figure 6:** a-f. Secondary yellow uranium encrustation in (a) black marble (b) highly altered marble (c) travertine (d) calcrete (e) Cr - rich plant molds in travertine (f) varicolored marble breccia embedded in travertine.

**Table 4:** Chemical composition of uranium minerals.

Type of sample	UO <sub>3</sub>	V <sub>2</sub> O <sub>5</sub>	CaO	Na <sub>2</sub> O	K <sub>2</sub> O	SiO <sub>2</sub>	CO <sub>2</sub>	U-Minerals
Marble	81.9-83.5		13.1-13.3					V
Marble/travertine	73.1-77.0	21.3-27.1						F
Marble/travertine	65.5-69.9	18.3-20.0	11.7-14.0					Mt
Marble/travertine	56.3-60.2	31.8-36.5	6.5-10.2					Mt
Travertine	68.8-69.2	24.1-24.3		6.0-6.1				S
Marble/ Secondary veins	64.2-71.3	18.6-23.1			3.8-5.9			C
Travertine	57.6-71.5	21.4-27.8	1.7-9.1	3.1-5.5				SS (Mt-S)
Travertine	38.5-41.4	13.1-13.5		2.9-3.3			41.1-43.9	?
Calcrete	62.3-68.5	19.9-21.6	8.8-11.4			1.6-3.0		?
Calcrete	37.4-42.8	15.1-18.2	35.8-38.1			6.2-6.3		?
Calcrete	52.7-55.2	17.2-18.8	6.1-9.2			6.1-10.4	14.5-18.9	?
Calcrete	38.8-58.0	13.1-18.9	2.5-14.8	1.4-5.5		1.1-5.7	6.0-18.2	?

• Mt = Metatyuyamunite  $\text{Ca}(\text{UO}_2)_2\text{V}_2\text{O}_8 \cdot 3(\text{H}_2\text{O})$

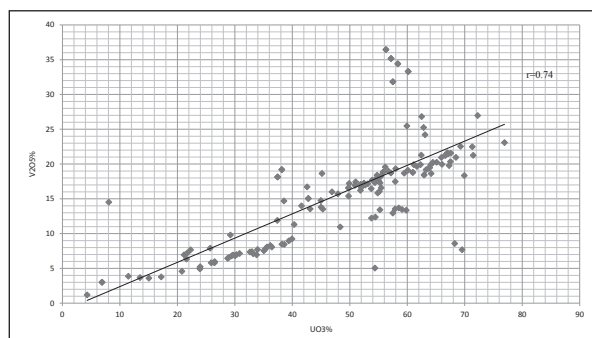
• S = Strelkinite  $\text{Na}_2(\text{UO}_2)_2\text{V}_2\text{O}_8 \cdot 6(\text{H}_2\text{O})$

• C = Carnotite  $\text{K}_2(\text{UO}_2)_2\text{V}_2\text{O}_8 \cdot 3(\text{H}_2\text{O})$  – restricted to K-rich marble

• F = Ferganite  $\text{U}_3(\text{VO}_4)_2 \cdot 6\text{H}_2\text{O} ?$

• V = Vorlanite  $(\text{CaU}_6)\text{O}_4$

• SS (Mt-S) = Solid solution between metatyuyamunite -strelkinite

**Figure 7:** EDS results: UO<sub>3</sub> vs V<sub>2</sub>O<sub>5</sub> correlation of the uranium minerals.

## 4. Discussion

### 4.1. Source of U and V

The results have indicated the association of uranium and vanadium in the surficial deposits of central Jordan. The main sources of redox sensitive trace elements U, Cr, Ni, V and Zn in central Jordan is the bituminous marl and the underlying phosphorites. Organic matter and sulfides enable the reducing environment. The marine phosphorite beds immediately below the bituminous marl are enriched in U up to 200 ppm (Khoury, 2006; Abed, 2012; El-Hasan, 2008; Khoury et al., 2014). Uranium, as well as Cr, Ni, V and Zn are trace elements that precipitate in suboxic and fully anoxic bottom-water environments and accumulate in marine sediments, such as oil shale (Piper and Calvert 2009). The same conditions resulted in the concentration of trace elements in the form of sulfides and selenides in the bituminous marl (Al Nawafleh, 2007). Organic acids may increase the solubility of U in the bituminous marl, but its mobility may be limited by the formation of slightly soluble precipitates (e.g., phosphates and oxides) and by adsorption on clay minerals and organic matter (Kim, 1993; Read et al., 1993). Sr and U are hosted by calcite and francolite structures as a result of substitution for Ca. The sulfides and selenides were formed during the early diagenetic reducing stage (Khoury and Nassir, 1982 a and b; Milodowski, et al, 1998). The bituminous marl in central Jordan is characterized by unusual high concentrations of

U, Cr, Ni, V, Zn, and Zr (Table 3). The average U content is 33 ppm. Uranium and vanadium are mostly associated with francolite structure and are adsorbed onto the organic material and the clay minerals.

The spontaneous combustion of the bituminous marl in central Jordan as indicated by Khoury and Nassir (1982b) is responsible for the formation of the varicolored marble (pyrometamorphic rocks). The chemical composition of the combusted bituminous rocks of central Jordan remained the same with a mass loss of 30% as indicated in the equivalent bituminous rocks of the mottled zone (Gellerhe et al., 2012). Combustion has further enriched the metamorphic rocks with trace elements. The source rock for uranium mineralization in central Jordan is the combusted bituminous marl (varicolored marble). Meteoritic water similar to the active system in Maqarin, north Jordan is responsible for the travertine and calcrete precipitation in central Jordan (Khoury, 2012). The groundwater discharges today in Maqarin, is characterized by high hydroxide alkalinity (pH ~ 12.7), and saturation with calcium sulfate and high concentrations of redox sensitive trace elements and precipitates soft travertine (Khoury et al., 1992). The original protolith (the bituminous rocks) in Maqarin is highly enriched in trace elements and is equivalent from the stratigraphical, lithological, mineralogical and chemical point of view to those in central Jordan and the mottled zone. All the travertine deposits in Maqarin area are recent and are precipitating as a result of the reaction of the hydroxide-sulfate waters with atmospheric CO<sub>2</sub>.

The same mechanism has prevailed in an ancient system in central Jordan where travertine and caliche deposits overlie the varicolored marble. The travertine is an evidence for discharges of hyperalkaline groundwater in the past (Khoury, 2012; Khoury et al., 2014). Thick travertine deposits were formed during wet periods in the low topography areas, and calcrete was formed later during dry period. The dry climate has contributed to increase metals concentration such as U, Cr, Ni, V and Zn.

The widely distributed brecciated varicolored marbles embedded in the travertine cement indicates a wet pluvial period. The presence of gypsum, fluorite and halite in the calcrete indicate a dry evaporation period.

#### 4.2. Uranium mineralization

The U content of the rocks is variable and reaches up to 419 ppm in the whole rock trench samples (Table 3). Both U and V are associated together as uranyl vanadate phases in most of the studied yellow crystals as (Table 4). The low correlation coefficient between U and V in the whole rock samples (Fig. 8) is related to the presence of V in the structure of sulphates, phosphates, REE hosted minerals and Cr-smectite. Uranium solubility in solution is predominantly controlled by the oxidation-reduction potential and pH (Murphy and Shock, 1999). Uranium mineralization in the travertine and calcrete is favored by the presence of source rocks of uranium and vanadium, and oxidizing alkaline circulating water. The uranyl ion is an oxyanion of uranium in the oxidation state +6, with the chemical formula  $[\text{UO}_2]^{2+}$ . Uranium +6 is considerably more soluble than uranium +4 and is highly mobile as hexavalent uranyl ion ( $\text{UO}_2^{2+}$ ) under oxidizing conditions (Langmuir, 1978; 1997). Under reducing conditions, uranium (+4) complexes with hydroxide or fluoride are the only dissolved species (Gascoyne, 1992). The precipitation of uranium (+4) under reducing conditions is the dominant process leading to naturally enriched zones of uranium in the subsurface (Osmond and Cowart, 1992). The hydroxide  $\text{UO}_2(\text{OH})_2$  dissolves in strongly alkaline solution to give hydroxy complexes of the uranyl ion. As pH increases the hydroxide species  $[(\text{UO}_2)_2(\text{OH})_2]^{2+}$  and  $[(\text{UO}_2)_3(\text{OH})_5]^{+}$  form before the precipitation of  $\text{UO}_2(\text{OH})_2$  (Hagberg, et al., 2005). The association of vanadium with uranium in the secondary uranium minerals needs an oxidizing environment to oxidize dissolved  $\text{V}^{4+}$  to  $\text{V}^{5+}$ . Complexing agents such as vanadium compounds are necessary to fix the uranyl-ion and vanadate to precipitate very low solubility uranium minerals in the form of uranyl vanadates (Battey et al., 1987; Brookins, 1988). Hydroxyl vanadate  $\text{VO}_3\text{OH}^{-5}$  is the dominant complex under alkaline conditions.

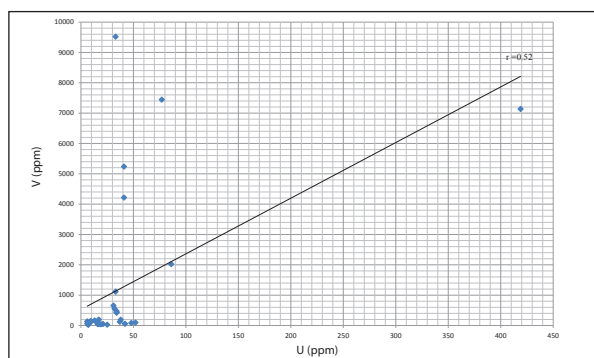


**Figure 8:** U values (ppm) plot versus V values (ppm) in the whole rock samples (Table 3).

The combustion of the organic rich source rock has accelerated leaching out the redox sensitive trace elements among others in the circulating highly alkaline water. The highly altered varicolored marble with its complex mineralogy shows yellow secondary U-minerals as encrustations and/or filling the veins, weakness zones and voids with other hydrous

silicates (Nassir and Khoury, 1982; Khoury and Nassir 1982a and b; Khoury, 2012). Uranium and vanadium with other trace elements were leached out from the varicolored marble and were carried out by the oxidizing alkaline circulating water. Such conditions are indicated by the presence of relatively high levels of Sr, Cr, Ti, Mn, Ni, Zn, V, Zr, Cl, F, Se and REE in the Pleistocene-Recent carbonate sediments (Khoury, et al., 1984). The absence of Cs in the surface uranium phases indicates a low temperature solution (Healy and Young, 1998). U-levels up to 160 ppm were found in opaline phases adjacent to open voids (Hyslop, 1998). The yellow uranium phases are present in patches at the surface and along weakness zones in the travertine and caliche.

The oxidizing environment of the alkaline water in central Jordan is indicated by the presence of abundant  $\text{Cr}^{6+}$  mineralization ( $\text{Cr}^{6+}$ -bearing ettringite and hashemite). Uranium +6 is considerably more soluble than uranium +4 and is highly mobile as hexavalent uranyl ion ( $\text{UO}_2^{2+}$ ) under oxidizing conditions (Langmuir, 1978; 1997). Oxidizing alkaline circulating water is a prerequisite to oxidize dissolved  $\text{V}^{4+}$  to  $\text{V}^{5+}$ , and to mobilize uranium as uranyl complexes thereby establishing the conditions required for the precipitation of uranium vanadate minerals as strelkinite and tyuyamunite and carnotite (Battey et al., 1987; Dahikamp, 1993). Complexing agents such as vanadium compounds are necessary to fix the uranyl-ion and vanadate to precipitate very low solubility uranium minerals in the form of uranyl vanadates as strelkinite and metatyuyamunite. The solid solution series between strelkinite and metatyuyamunite is dependent on the Ca /Na ratio in solution. Carnotite precipitates are dependent on the availability of K in the circulating water. The composition of other unidentified U-V phases was dependent on the solution chemistry. In the absence of uranyl vanadates complexes in the alkaline conditions, soluble uranyl-carbonate complexes as uranyl carbonates  $\text{UO}_2(\text{CO}_3)_2^{2-}$  are the most probable to dominate (Langmuir, 1978; 1997; Battey, et al., 1987; Brookins, 1988). After the removal of  $\text{Ca}(\text{OH})_2$  from the alkaline water and the precipitation of calcite, uranium carbonates as urancalcrite could precipitate.

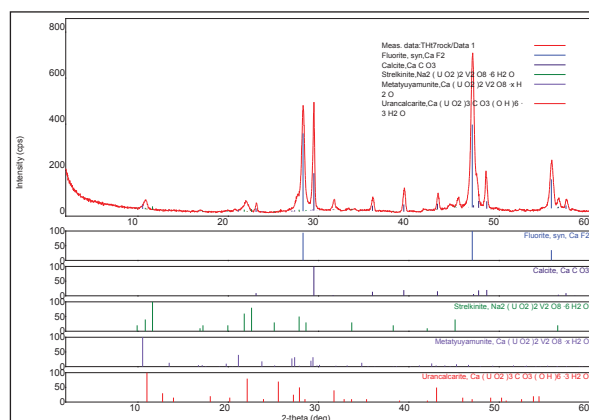


**Figure 9:** XRD results of a representative sample of uranium yellow encrustations.

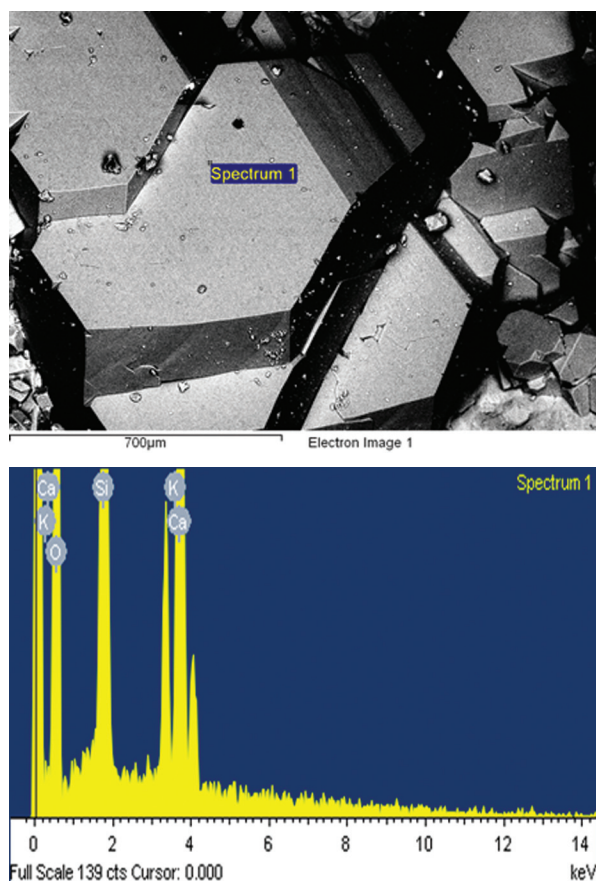


**Figure 10:** SEM –EDX photomicrograph of secondary K-rich apophyllite associated with brown marble.

## 5. Conclusion

Unusual surface uranium deposits cover large areas in central Jordan. Uranium distribution is inhomogeneous and follows porous weakness zones of chalk marl/travertine and caliche/top soil deposits. The source of uranium and other redox sensitive metals Cr, Ni, V, Zn, and Zr is the combusted bituminous marl (varicolored marble). The high concentration of these metals is reflected by the chemistry of secondary low temperature minerals hosted by the travertine and caliche. Quaternary travertine and caliche in central Jordan are the fossilized products of ancient hyperalkaline oxidized groundwater discharges that prevailed during wet/dry periods in the Peistocene –Recent time.

The main surficial secondary uranium minerals in central Jordan are strelkinite and metatuyamunite with all possible solid solution between the two end members. Other unidentified U-V silicates and carbonates possibly were precipitated under the same conditions.

## Acknowledgment

The author would like to thank the Deanship of Scientific Research at the University of Jordan for their financial support of supporting my sabbatical year at the Department of Earth Sciences, University of Ottawa, Canada. Thanks are extended to Prof. Ian Clark and Late Prof. Andre Lalonde for supporting the analytical work in the different laboratories.

The work entitled “The geochemistry of surficial uranium deposits from central Jordan” was accomplished during the sabbatical year 2012/2013. Part of the analytical work was done at the laboratories of the Federal Institute for Geosciences and Natural Resources, Hanover, and the Department of Geology, Greifswald University, Germany.

## References

- [1] Abed, A., 2012. Review of uranium in the Jordanian phosphorites: Distribution, genesis and industry. *Jordan Journal of Earth and Environmental Sciences* 4, (2) 35-45.
- [2] Abed, A.M., Fakhouri, K., 1996. On the chemical variability of phosphatic particles from Jordanian phosphorite deposits. *Chemical Geology* 131, 1–13.
- [3] Alnawafleh, H., 2007. Geological factors controlling the variability of Maastrichtian bituminous rocks in Jordan. Unpublished Ph.D thesis. The University of Nottingham, England. 279P.
- [4] Alqudah, M., Hussein, M., Podlaha, O., Boorn, S., Kolonic S., and Mutterlose, J. 2014. Calcareous nannofossil biostratigraphy of Eocene oil shales from central Jordan. *GeoArabia*, 19, (1), 117-140.
- [5] Alqudah, M., Hussein, M., Podlaha, O., Boorn, S., Podlaha, O., and Mutterlose, J. 2015. Biostratigraphy and depositional setting of Maastrichtian Eocene oil shales from Jordan, *Marine and Petroleum Geology*. (In Publication)
- [6] Barjous, M., 1986. The geology of Siwaqa, Bull. 4, NRA, Amman – Jordan.
- [7] Battey, G., Miezitis, Y., and McKay, A., 1987. Australian Uranium Resources, Bureau of Mineral Resources, Resource Report No. 1, Australia Government Publishing Service, Canberra.
- [8] Brookins, D., 1988. Eh-PH diagrams for geochemistry. Springer-Verlag Berlin.
- [9] Clark, I. D., Fontes, J-Ch., and P. Fritz, 1992. Stable isotope disequilibria in travertine from high pH waters: laboratory investigations and field observations from Oman. *Geochimica Cosmochimica Acta*, 56: 2041 - 2050.
- [10] Clark, I., Firtz, P. Seidlitz, H., Khoury, H., Trimborn, P., Milodowski, T., and Pearce, J., 1993. Recarbonation of metamorphosed marls, Jordan. *App. Geochem.* 8: 473 - 481.
- [11] Cuney, M., 2009. The extreme diversity of uranium deposits. *Miner Deposita* 44:3–9
- [12] Dahikamp, F.J., 1993. Uranium Ore Deposits. Springer-Verlagm, Berlin Heidelberg. p 460.
- [13] Gascoyne, M., 1992. Geochemistry of the actinides and their daughters. In *Uranium-series Disequilibrium: Applications to Earth, Marine, and Environmental Science* (ed. M. Ivanovich and R. S. Harmon), 34-61. Clarendon Press.
- [14] El-Hasan, T. (2008): Geochemistry of the redox-sensitive trace elements and its implication on the mode of formation of the Upper Cretaceous oil Shale, Central Jordan. *Neues Jahrbuch fuer Geologie und Palaeontologie Abh.* 249(3): 333-344.
- [15] Gellerhe, Y., Burg A., Halicz, L., Kolodny Y., 2012. System closure and isochemistry during the Mottled Zone event, Israel. *Chemical Geology*. 334, 102-115.
- [16] Hagberg, D., Karlström, G., Roos BO., Gagliardi, L., 2005. "The Coordination of Uranyl in Water: A Combined Quantum Chemical and Molecular Simulation Study". *J. Am. Chem. Soc.* 127 (41): 14250–14256.
- [17] Healy, R., and Young, J., 1998. Mineralogy of U-bearing marls from The Jordanian desert. Unpublished Report for Cameco Corporation, Canada. A report submitted to the Natural Resources Authority, Amman, Jordan.
- [18] Hyslop, E., 1998. Uranium distribution and whole rock geochemistry. In phase II report (Nirex S/98/003) edited by C.M. Linklater.
- [19] IAEA, 2009. World distribution of uranium deposits (UDEPO) with uranium deposit classification. IAEA- Vienna, TECDOC-1629.
- [20] Jaser, D., 1986. The geology of Khan Ez Zabib, Bull. 3, NRA, Amman, Jordan
- [21] Khoury, H. N., 1989. Mineralogy and petrology of the opaline phases from Jordan. *N. Jb. Miner. Mh.*, 10, 433-440.
- [22] Khoury, H., 2006. *Industrial rocks and minerals in Jordan* (second edition). Publications of the University of Jordan, Amman.
- [23] Khoury, H. N., 2012. Long-Term Analogue of Carbonation in Travertine from Uleimat Quarries, Central Jordan. *Environmental and Earth Science*. 65:1909-1916.

- [24] Khoury, H., and Al-Zoubi, A. 2014. Origin and characteristics of Cr-smectite from Suweileh area, Jordan. *Applied Clay Science*, 90, 43–52.
- [25] Khoury, H., Mackenzie, R., Russell, J., and Tait, J., 1984. An iron-free volkonskoite. *Clay Minerals*, 19: 43-57.
- [26] Khoury, H., and Nassir, S., 1982a. A discussion on the origin of Daba – Siwaqa marble, *Dirasat*, 9: 55-56.
- [27] Khoury, H., and Nassir, S., 1982b. High temperature mineralization in Maqarin area, Jordan. *N.Jb.Mineral.Abh.*, 144, 187-213.
- [28] Khoury, H., and Milodowski, A., 1992. High temperature metamorphism and low temperature retrograde alteration of spontaneously combusted marls. The Maqarin cement analogue. *Water Rock Interaction*, Kharaka & Maest (Eds), Rotterdam. 1515-1518.
- [29] Khoury, H., Pearce, J., and Hyslop, E., 1992. In Phase I. Nagra Technical Report, NTB 9-10, Nagra, Wetingen, Switzerland.
- [30] Khoury, H. N., Salameh, E. M. and Clark I. D. 2014. Mineralogy and origin of surficial uranium deposits hosted in travertine and calcrete from central Jordan. *Applied Geochemistry*, 43, 49–65.
- [31] Khoury H. N., Salameh, E., Clark, F., Fritz, R., Bajjali, W., Milodowski, A., Cave, M., and Alexander, W., 1992. A natural analogue of high pH waters from the Maqarin area of northern Jordan 1: Introduction to the site. *J. Geochem. Explor.* 46, 117-132.
- [32] Kim, J. I., 1993. The chemical behaviour of transuranium elements and barrier functions in natural aquifer systems. *Mater. Res. Soc. Symp. Proc.*, 294, 3-21.
- [33] Langmuir, D., 1978. Uranium solution-mineral equilibria at low temperatures with applications to sedimentary ore deposits. *Geochim. Cosmochim. Acta* 42, 547-569.
- [34] Langmuir D., 1997. *Aqueous environmental chemistry*. Prentice Hall.
- [35] Mckay, A., and Miezitis, Y., 2001. Australia's uranium resources, geology and development of deposits, AGSO — Geoscience Australia Resource Report 1.
- [36] Milodowski, A., Hyslop, E., Pearce, J., Wetton, P., Kemp, S., Longworth, G., Hodginson, E., and Hughes, C., 1998. Mineralogy and Geochemistry in Phase III SKB Technical Report. TR-98-04. PP401.
- [37] Murphy, W. M., and Shock E. L., 1999. Environmental Aqueous Geochemistry of Actinides. In *Uranium: mineralogy, geochemistry and the environment*, Mineralogical Society of America. 38 (ed. P. C. Burns and R. Finch), 221-254.
- [38] Nassir, S., and Khoury, H., 1982. Mineralogy, petrology, and origin of Daba-Siwaqa marble, Jordan. *Dirasat*. 9: 107-130.
- [39] Osmond J. K. and Cowart J. B., 1992. Ground water. In *Uranium-series Disequilibrium: Applications to Earth, Marine, and Environmental Science* (ed. M. Ivanovich and R. S. Harmon), (Gascoyne, 1992). 290-333. Clarendon Press.
- [40] Powell, J.H., 1989. Stratigraphy and sedimentology of the Phanerozoic rocks in central and southern Jordan. *Bull. 11, Geology Directorate, natural resources Authority (Ministry of Energy and Mineral resources) Amman, Part B: Kurnub, Ajlun and Belqa group*, 161.
- [41] Powell, J. H., Moh'd, B.K., 2011. Evolution of Cretaceous to Eocene alluvial and carbonate platform sequences in central and south Jordan. *GeoArabia*, 16, 4, 29-82.
- [42] Read, D., Bennett, D.G., Hooker, P.J., Ivanovich, M., Longworth, G., Milodowski, A.E., Noy, D.J., 1993. The migration of uranium into peat-rich soils at Broubster, Caithness, Scotland. *J. Contam. Hydrol.*, 13, 291-308.
- [43] Piper, D.Z. and Calvert, S.E., 2009. A marine biogeochemical perspective on black shale deposition. *Earth Science Reviews*, 95, 63–96.
- [44] Salameh, E., Khoury, H., and Schneider, W., 2006. Jebel Waqf as Suwwan, Jordan: a possible impact crater – a first approach. *Z. dt. Geowiss.* 157/3, p. 319-325.
- [45] Salameh, E., Khoury, H., Reimold, W., and Schneider, W., 2008. The first large meteorite impact structure discovered in the Middle East: Jebel Waqf as Suwwan, Jordan. *Meteoritics and Planetary Science*. 43, Nr 10, 1681-1690.
- [46] Sharygin, V.V., Sokol, E.V., Vapnik, Ye., 2008. Minerals of the pseudobinary perovskite-brownmillerite series from combustion metamorphic lamite rocks of the Hatrurim Formation (Israel). *Russian Geology and Geophysics*. 49, 709-726.
- [47] Sokol, E.V., Novikov, I.S., Vapnik, Ye., Sharygin, V.V., 2007. Gas fire from mud volcanoes as a trigger for the appearance of high-temperature pyrometamorphic rocks of the Hatrurim Formation (Dead Sea area). *Doklady Earth Sciences*. 413A, 474-480.
- [48] Sokol, E.V., Novikov, I.S., Zateeva, S.N., Sharygin, V.V., Vapnik, Ye., 2008. Pyrometamorphic rocks of the spurrite-merwinite facies as indicators of hydrocarbons discharge zones (the Hatrurim Formation, Israel). *Doklady Earth Sciences*. 420, 608- 614.
- [49] Sokol, E., Novikov, I., Zateeva, S., Vapnik, Ye., Shagam, R., Kozmenko, O., 2010. Combustion metamorphism in the Nabi Musa dome: new implications for a mud volcanic origin of the Mottled Zone, Dead Sea area. *Basin Research*. 22, 414-438.
- [50] Vapnik, Ye., Sharygin, V.V., Sokol, E.V., Shagam, R., 2007. Paralavas in a combustion metamorphic complex: Hatrurim Basin, Israel. *Geological Society of America, Reviews in Engineering Geology*. 18, 133-154.